RASID: A Robust WLAN Device-free Passive Motion Detection System

Ahmed E. Kosba
Dept. of Comp. and Sys. Eng.
Faculty of Engineering,
Alexandria University, Egypt
Email: ahmed.kosba@alexu.edu.eg

Ahmed Saeed
Wireless Research Center
Egypt-Japan Univ. of Sc. & Tech. (E-JUST)
Alexandria, Egypt
Email: ahmed.saeed@ejust.edu.eg

Moustafa Youssef
Wireless Research Center
Egypt-Japan Univ. of Sc. & Tech. (E-JUST)
& Alexandria University, Alexandria, Egypt
Email:moustafa.youssef@ejust.edu.eg

Abstract—WLAN Device-free passive (*DfP*) indoor localization is an emerging technology enabling the localization of entities that do not carry any devices nor participate actively in the localization process using the already installed wireless infrastructure. This technology is useful for a variety of applications such as intrusion detection, smart homes and border protection.

We present the design, implementation and evaluation of *RASID*, a *DfP* system for human motion detection. *RASID* combines different modules for statistical anomaly detection while adapting to changes in the environment to provide accurate, robust, and low-overhead detection of human activities using standard WiFi hardware. Evaluation of the system in two different testbeds shows that it can achieve an accurate detection capability in both environments with an F-measure of at least 0.93. In addition, the high accuracy and low overhead performance are robust to changes in the environment as compared to the current state of the art *DfP* detection systems.

Keywords-Anomaly detection, device-free passive localization, motion detection systems, robust device-free localization.

I. INTRODUCTION

The increasing need for context-aware information and the rapid advancements in communication networks have motivated significant research effort in the area of location-based services. This effort resulted in the development of many location determination systems, including the GPS system [1], ultrasonic-based systems [2], infrared-based (IR) systems [3], and radio frequency-based (RF) systems [4]. Moreover, motion detection systems, that aim at detecting the motion of an entity carrying a device, were also developed [5]–[13]. These systems require the tracked entity to carry a device that participates in the localization process. Thus, we refer to them as device-based systems.

Motivated by the wide use of wireless LANs for indoor communication, we recently introduced the concept of device-free passive *DfP* localization [14] which enables the detection and tracking of entities that do not carry any devices nor participate in the localization process. This concept depends on the fact that the presence and motion of entities in an RF environment affects the RF signal strength, especially when dealing with the 2.4 GHz band which is used in different IEEE standards such as 802.11b and 802.11g (WiFi). Different *DfP* algorithms were proposed for
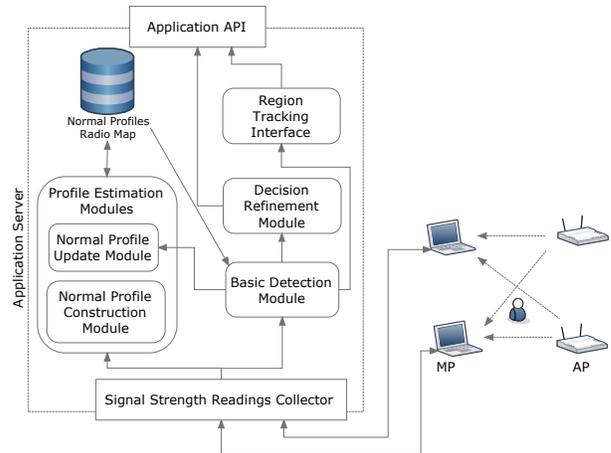

Figure 1. *RASID* system architecture.

detection [14], [15] and tracking [14], [16]–[18] of entities in indoor environments. Our focus in this paper is on the detection problem.

In particular, we address the problem of designing a low-overhead, accurate, and robust *DfP* motion detection system. We introduce the *RASID* system that provides a software only solution on top of the already installed wireless networks enabling a wide set of applications including intrusion detection, border protection, and smart homes. As a typical *DfP* system, *RASID* consists of signal transmitters, such as access points (APs), signal receivers or monitoring points (MPs), such as standard laptops[1], and an application server which collects and processes information about the received signals from each MP. The application server contains the main system modules responsible for performing the detection function (Figure 1).

Our research on *RASID* is motivated by several factors: First, the technologies that can be used to provide the desired detection capability (e.g. cameras [19], IR sensors, radio tomographic imaging [20], pressure sensors [21], etc) share the requirement of installing special hardware. In addition, cameras and IR sensors are limited to line-of-sight vision

---

[1]Note that it is also possible to use the access points themselves as monitoring points.

and thus the cost of covering an area might be prohibitive. Moreover, regular cameras fail to work in the dark or in the presence of smoke. *RASID* avoids these drawbacks by using the already installed wireless infrastructure without installing any special hardware. It also makes use of the fact that RF waves do not require LOS for propagation.

From another perspective, the previously proposed WLAN *DfP* detection techniques [14], [15] provide good performance under strong assumptions, which limit their application domain. For example, they are not robust to changes in the environment. That is they do not adapt to changes in the environment, e.g. humidity and temperature changes. Moreover, their parameters need to be changed as the deployment area changes. In addition, the technique proposed in [15] requires the construction of a human motion profile which leads to high overhead inside large-scale environments. The cost of this technique may be prohibitive, as it requires access to all areas of a building which might include restricted or private areas and requires several hours of calibration. Finally, all techniques were either evaluated in controlled environments, e.g. [14], or in small-scale real environments, e.g. [15].

In order to achieve its objectives, *RASID* uses a statistical anomaly detection technique to detect motion inside indoor environments [22]. *RASID* only constructs a non-parametric profile for the signal strength readings received at the MPs when there is no human activity during a short training phase of only two minutes, leading to minimal deployment overhead. *RASID* also employs techniques for continuously updating its silence profile to adapt to the environment changes. The system also applies a decision refinement procedure in order to reduce the false alarms due to the signal noise. Furthermore, *RASID* also provides an interface by which the regions of activity can be identified. We evaluate the system in two different large-scale environments rich in multi-path and compare *RASID* to the state-of-the-art *DfP* detection techniques [14], [15]. Our results show that *RASID* achieves its goals of high accuracy in both environments with minimal deployment overhead. In addition, it is robust to changes in the environment.

In summary, the contributions of this paper are four-fold:

- We present the architecture and implementation of *RASID*: a system that provides robust device-free motion detection along with techniques for adapting to environment changes and handling the wireless signal noise.
- We analyze different signal strength features that can be used for detection and identify the most promising one.
- We evaluate the system in two different large-scale real testbeds and compare it to the state-of-the-art *DfP* detection techniques.
- We present a comparison of parametric and non-parametric approaches for system operation.

The rest of this paper is organized as follows: Section II reviews related work. Section III presents the *RASID* system architecture and operation. Section IV presents the experimental evaluation of *RASID* and a comparison with other techniques. Section V compares the non-parametric approach used in the system to a parametric analytical model for the system operation. Finally, Section VI concludes the paper and discusses future work.

II. RELATED WORK

Motion Detection in device-based systems has been an active field of research. Several approaches have been proposed to detect the motion of an entity carrying a device either with the use of special hardware like accelerometers or motion sensors [6], [7], or by using the existing network infrastructures like wireless networks [9], [11] and GSM [12].

From the device-free perspective, multiple technologies can be used to provide the desired capabilities including: ultra-wide band radar [23], computer vision [19], physical contact-based systems [21] and radio tomographic imaging [20]. Other technologies include the usage of wireless sensors for tracking transceiver-free objects [24]. Those technologies share the requirement of installing special hardware to handle the device-free functionalities. In addition, cameras and IR sensors are limited to line-of-sight vision and thus they require a high cost deployment to cover all site regions. Regular cameras may also fail to work in the absence of light or the presence of smoke. Ultra-wide band radar based techniques also suffer from high complexity. Moreover, some techniques can require high density to provide full coverage like radio tomographic imaging and physical contact-based systems using pressure sensors.

WLAN device-free passive systems aim to avoid the above drawbacks by using the already available wireless infrastructure. The concept of device-free passive detection and tracking using WLANs was first proposed in [14] with a large number of applications including intrusion detection, border protection [25], smart homes, and traffic estimation [26]. Techniques for *DfP* detection [14], [15] and tracking [14], [16]–[18], [27] were introduced. The proposed techniques for the detection capability are either based on time-series analysis, like the moving average and moving variance techniques proposed in [14], or based on classification using the maximum likelihood estimation [15]. These techniques are not robust to changes in the environment. In addition, some techniques require the construction of a human motion profile which is a high overhead process for large-scale environments [15]. Moreover, these techniques were either evaluated in controlled environments, e.g. [14], or in small-scale real environments, e.g. [15].

RASID addresses these drawbacks using statistical anomaly detection techniques along with other techniques devised for adapting to environment changes and refining

its decision. This enables *RASID* to achieve low deployment overhead, high accuracy, and high robustness.

III. THE RASID SYSTEM

In this section, we give the details of the *RASID* system. We start by an overview of the system architecture followed by the details of the system modules.

A. System Overview

Figure 1 gives an overview of the system architecture. The modules of the proposed system are implemented in the application server that collects samples from the monitoring points and processes them. The system works in two phases: 1) A short *offline* phase, during which the system studies the signal strength values when no human is present inside the area of interest to construct what we call a "normal or silence profile" for each stream. The profiles of all streams are constructed concurrently in that short phase. 2) A *monitoring* phase, in which the system collects readings from the monitoring points and decides whether there is human activity (anomalous behavior) or not based on the information gathered in the offline phase. It also updates the stored normal profile so that it can adapt to environment changes. Finally, a decision refinement procedure is applied to further enhance the accuracy.

The *Normal Profile Construction Module* constructs the initial silence profiles based on a short, typically two minutes, training sample taken when there is no human motion present in the area of interest. (Section III-C)

The *Basic Detection Module* examines each stream readings in the monitoring phase and decides whether there is an anomalous behavior or not. This operation is applied to each stream independently. It also assigns an anomaly score to each stream to express the intensity of the anomalous behavior. (Section III-E)

The *Normal Profile Update Module* updates the normal profiles constructed in the offline phase in order to adapt to changes in the environment. (Section III-F)

The *Decision Refinement Module* applies heuristic methods to refine the decision generated by the basic detection module to reduce the false alarm rates. (Section III-G)

The *Region Tracking Interface* provides an interface that visualizes the output of the above modules. This interface enables the user to identify the detected events and provides the regions of the moving entities. (Section III-H)

We start by giving the mathematical notations followed by the details of the different modules.

B. Mathematical Notations

Let k be the number of streams, which is equal to the number of APs times the number of MPs. Let $s_{j,t}$ denote the received signal strength (RSS) reading for a stream j that is received at a time instant t. The system studies the
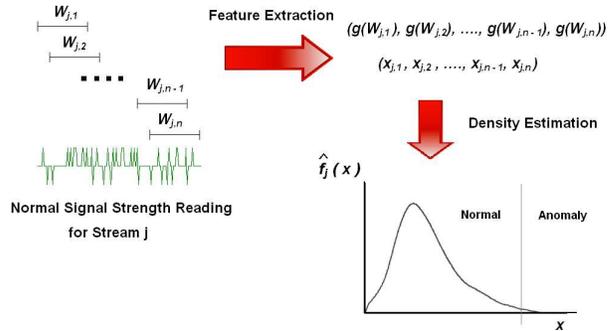

Figure 2. Illustration of the normal profile construction.

behavior of a sliding window $W_{j,t}$ of size l that ends at time t, i.e. $W_{j,t} = [s_{j,t-l+1}, s_{j,t-l+2}, ..., s_{j,t}]$.

In order to study the behavior of the sliding windows, each sliding window $W_{j,t}$ is mapped to a single *feature* or value $x_{j,t}$ through a function g. For example, if the mean is the selected feature, then $g(W_{j,t}) = \frac{1}{l} \sum_{i=1}^{l} s_{j,t-l+i}$. Two types of features can be considered: measures of central tendency, such as the mean, and measures of dispersion or variation, such as the variance.

C. Normal Profile Construction

The purpose of the Normal Profile Construction Module is to construct a normal profile, capturing the received signal strength characteristics when there is no human in the area of interest. This is used later by other modules to detect anomalies. This module runs in the offline phase. It extracts the feature values from the sliding windows over the collected data and estimates its distribution. The density function of the feature values observed is estimated using non-parametric kernel density estimation[2]. This is done for each stream independently. Figure 2 illustrates the operation.

Formally, for a stream j, given a set of n sliding windows, each of length l samples, each window $W_{j,i}$ is mapped to a value $x_{j,i}$, where $x_{j,i} = g(W_{j,i})$. Assume f_j is the density function representing the distribution of the observed $x_{j,i}$'s, then given a random sample $x_{j,1}, x_{j,2}, ..., x_{j,n}$, the estimated density function $\hat{f}_j$ is given by [28]:

$$\hat{f}_j(x) = \frac{1}{nh_j} \sum_{i=1}^{n} V\left(\frac{x - x_{j,i}}{h_j}\right) \quad (1)$$

where h_j is the bandwidth and V is the kernel function. The choice of the kernel function is not significant for the results of the approximation [29]. Hence, we choose the Epanechnikov kernel as it is bounded and efficient to integrate:

---

[2]In Section V, we present the motivation for using a non-parametric approach by providing a performance comparison with a parametric modeling of the system operation.

$$V(q) = \begin{cases} \frac{3}{4}(1 - q^2), & \text{if } |q| \le 1 \\ 0, & \text{otherwise} \end{cases} \qquad (2)$$

Also, we used Scott's rule to estimate the optimal bandwidth [29]:

$$h_j^* = 2.345 \hat{\sigma}_j n^{-0.2} \qquad (3)$$

where $\hat{\sigma}_j$ is an estimate for the standard deviation for the $x_{j,i}$'s.

After estimating the density function for the feature values extracted from the sliding windows, critical bounds are selected so that if the feature values observed in the monitoring state exceed those bounds, the observed values are considered anomalous. Given a significance parameter α and assuming $\hat{F}_j$ is the CDF of distribution shown in Equation 1, if the feature is a measure of central tendency, which can deviate to the left or the right, then lower and upper bounds will be calculated such that the lower bound is $\hat{F}_j^{-1}(\alpha/2)$ and the upper bound is $\hat{F}_j^{-1}(1-\alpha/2)$. However, if the feature is a measure of dispersion, which can only deviate in the positive (or right) direction, then an upper bound is only needed and is equal to $\hat{F}_j^{-1}(1-\alpha)$. In the next subsection, we study different features that can be selected.

D. Feature Selection

As the system requires an offline phase before operation, to learn the behavior of the signal readings in the normal state, the selected feature for system operation should be resistant to possible environmental changes that may affect the stored data, e.g. temporal variations[3]. In addition, the selected feature should also be sensitive to the human motion to enhance the detection accuracy.

In this section, we compare two categories of features: central tendency measures and dispersion measures. The goal of this study is to identify the category that will be more promising for the system operation. For this study, we consider the mean as a central tendency measure, and the standard deviation as a measure of dispersion. We use the standard deviation, rather than the variance, as the variance is a squared measure, while the mean is not.

1) Sensitivity to human activity: The selected feature should be sensitive to human activity. To compare the two features, we use the Euclidean distance between the normalized histograms representing the silence and motion states. The Euclidean distance is defined as the square root of the sum of the squared distance between each corresponding histogram bin. The histograms are constructed over a two-minute period for each state using Testbed 1, which is discussed later in Section IV. Figure 3 shows the comparison versus different window sizes. The figure shows that the

---

[3]Our experiments show that the changes in the traffic load on the network do not affect the signal strength. Therefore, temporal variations here refer to changes in the physical environment that affect the signal strength.
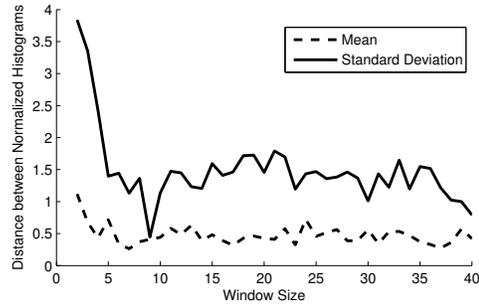

Figure 3. Distance between the features' normalized histograms for silence and motion states.
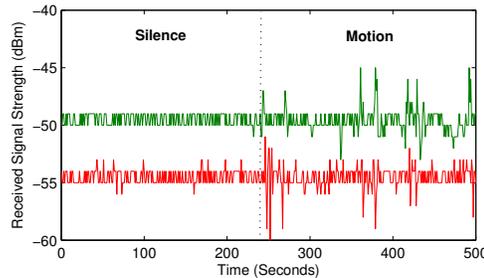

Figure 4. Illustrating the motion effect on wireless signals of two different streams.

distance between the histograms of the standard deviation is larger than the distance between the histograms of the mean. This indicates that the standard deviation feature is more discriminant of the human motion than the mean feature. This conclusion can be justified by observing the motion effect on typical wireless signals. Figure 4 provides a visualization of the raw signal strength for two different streams during silence and human motion periods. The figure shows that in the case of human motion, the fluctuations can be up or down around the normal/silence signal level, which leads to a limited effect on the mean as compared to the standard deviation.

2) Resistivity to temporal variations: As the proposed system requires a learning phase before operation, it is necessary to reduce the temporal variation effect on the stored profiles. To compare the two features, we use two different **silence** data sets collected two weeks apart. Figure 5 shows the results. The more similar the histograms, the more resistive the feature is to the introduced variations. The figure shows that the standard deviation feature is less affected by temporal variations. This is due to the fact that the standard deviation is a relative measure as it is calculated with respect to the mean, whereas the mean itself provides an absolute value that is more susceptible to be affected by changes in the conditions.

From this study, we conclude that the measures of dispersion, e.g. the standard deviation or variance, are more
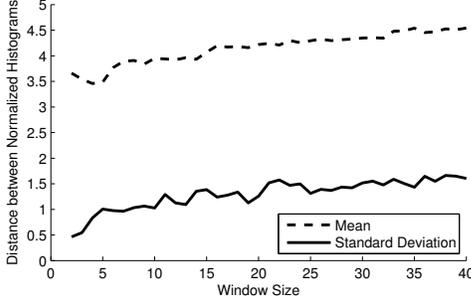
Figure 5. Distance between the features' normalized histograms for the two week-separated silence data.

suitable for our proposed system. For the rest of the paper, we use the sample variance as the selected feature.

E. Basic Detection Procedures

The Basic Detection Module runs during the monitoring phase. The purpose of this module is to detect signal strength anomalies, i.e. human presence, based on the normal profiles constructed during the offline phase. In particular, for a window of samples $W_{j,t}$ for stream j at a given time instant t, the module calculates the corresponding feature value $x_{j,t}$, i.e. the sample variance. A stream j is considered anomalous if $x_{j,t}$ is above a critical bound u_j. Given a significance parameter α and assuming $\hat{F}_j$ is the CDF of distribution shown in Equation 1, the upper bound u_j will be equal to the $100(1-\alpha)^{th}$ percentile of the CDF function, such that $u_j = \hat{F}_j^{-1}(1-\alpha)$.

The Basic Detection Module declares a global alarm when any stream is anomalous. This approach can lead to many false positives due to signal strength outliers. This is enhanced later by the Decision Refinement Module. The Basic Detection Module also calculates an anomaly score $a_{j,t}$ for each stream j to keep track of the significance of any anomalous activity. For a given window, $W_{j,t}$, the anomaly score, $a_{j,t}$, can be calculated as: $a_{j,t} = \frac{x_{j,t}}{u_j}$ where $x_{j,t}$ is the sample variance of the window and u_j is the critical value. This means that a detected anomaly will have a score greater than one and a silence window will have a score of less than one. The anomaly score is used by the Normal Profile Update and Decision Refinement modules to further enhance the accuracy.

In summary, the basic detection procedure requires two parameters: the window size l and the significance α. Analysis of both parameters is presented in Section IV-C.

F. Capturing Changes in the Environment: The Normal Profile Update Module

Due to the dynamic changes in the environment, the stored profiles may not capture the real normal state. Therefore, the systems needs to update the stored profiles during the online phase. The technique we employ for handling the update

process is based on continuously updating the estimated density in Equation 1, by adding $x_{j,t}$'s, that do not have high anomaly scores in average to it. In particular, during the monitoring phase, the system groups the consecutive $x_{j,t}$'s in disjoint groups of size l_{update}. The group that has an average anomaly score of less than one is added to the normal profile. The parameter l_{update} can be tuned to provide the desired performance. We quantify the effect of the l_{update} parameter in detail in Section IV-C2.

Adding new data to the normal profiles implies the need to give more weight to the recent data. Therefore, Equation 1 is modified to:

$$\hat{f}_j(x) = \frac{1}{h_j} \sum_{i=1}^{n} w_i V \left(\frac{x - x_{j,i}}{h_j} \right) \quad (4)$$

where $\sum_{i=1}^{n} w_i = 1$. We choose linear weights such that $w_i = \frac{i}{n(n+1)/2}$ (n is constant). We found that exponential weights do not provide good performance due to the high discrimination introduced between older and newer data.

G. The Decision Refinement Module

Typical wireless environments are noisy. This fact can cause many false alarms if the system generates alarms just based on a single stream. The goal of the Decision Refinement Module is to reduce the false alarm rate by fusing different streams.

Since the *Basic Detection Module* assigns an anomaly score to each detected event that expresses its significance, this can be leveraged to enhance the detection performance. The Decision Refinement Module studies the behavior of a global anomaly score a_t that is calculated by summing the individual anomaly scores for each stream. If a noticeable change in a_t occurs, based on a threshold, while at least one stream is anomalous, this implies the start of an anomalous behavior. The module makes use of the history of the activity state inside the environment through the usage of *exponential smoothing* to monitor the a_t in order to avoid the noisy samples, hence reducing the false alarm rate. It also implicitly makes use of the locality of human motion, meaning that the human will continue to affect the same stream and/or other streams near it, causing the sum of anomaly scores smoothed curve to have higher values during the motion period (Figure 6).

H. Region Tracking User Interface Module

The system provides an interface that provides information about the probable regions of the detected event. This is based on visualizing the anomaly degree of each stream enabling the user to identify the regions that probably have moving entities inside. This is done by coloring each pixel on the map according to its distance from each stream endpoints and according to the anomaly score of each
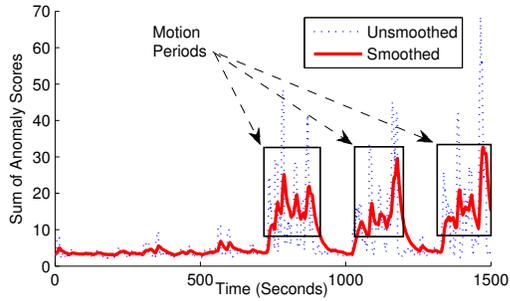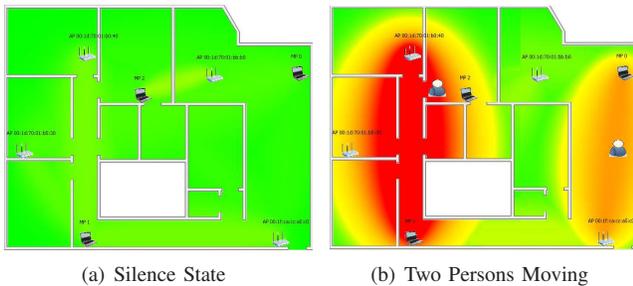
Figure 6. The behavior of the sum of anomaly scores for Testbed 1.

(a) Silence State　　　　(b) Two Persons Moving

Figure 7. The output of the Region Tracking Interface.

Figure 8. Testbed 1 layout and motion pattern.

(a) Floor 1　　　　(b) Floor 2

Figure 9. Testbed 2 layout and motion patterns.

stream. Figure 7 displays the output of this interface when two persons are moving inside a typical site, showing the true locations of the two persons.

IV. EXPERIMENTAL EVALUATION

In this section, we study the effect of the different parameters on the performance of the *RASID* system and compare it to the previous WLAN *DfP* detection techniques [14], [15].

A. Experimental Testbeds and Data Collection

We collected two sets of data to evaluate the system performance, each in a different testbed. The first testbed is an office of approximately 2000 ft^2. The second experiment was conducted in a two-floor home building where each floor was approximately 1500 ft^2. Both tesbeds were covered with typical furniture. For both testbeds, we used four Cisco Aironet 1130AG series access points and used three DELL laptops equipped with D-Link AirPlus G+ DWL-650+ Wireless NICs as MPs. The access points were operating on different channels. The experiments were conducted in typical IEEE 802.11b environments. Figures 8 and 9 show the layouts of both experiments.

For the data collection, sets of normal (silence) state readings and continuous motion readings were collected for each testbed. A total of about one hour and 15 minutes of data was collected for each testbed with a sampling rate of one sample per second using the active scanning technique [4]. For Testbed 1, this includes three motion sets, while
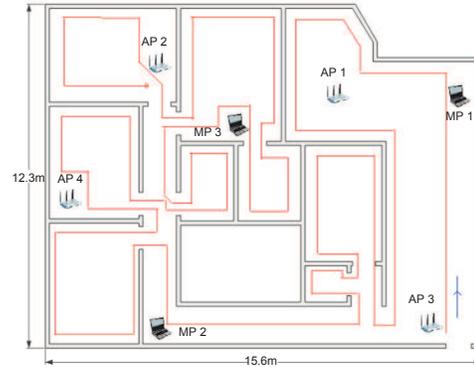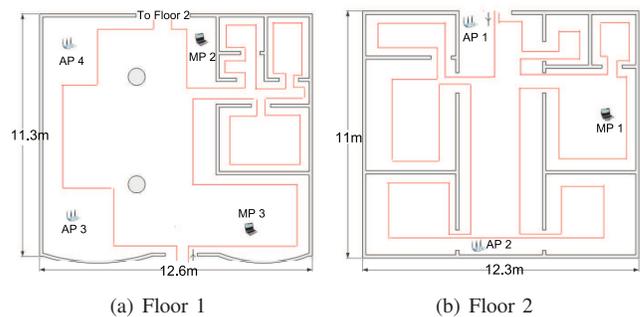
for Testbed 2, this includes two motion sets. A motion set covers the entire area of the testbed, as shown in figures 8 and 9, and represents the motion of a single person walking normally around the site without any stops.

For system evaluation, extreme conditions were employed: The training period is chosen to be only the first two minutes of the entire data collected with the absence of human motion. In addition, only one person moved in the area of interest. More people in the area of interest will lead to higher variance [30] and hence better detection. Therefore, the reported results present a lower bound on the performance of the *RASID* system.

B. Evaluation Metrics

We used three metrics to analyze the detection performance: the false positive (FP) rate, the false negative (FN) rate and the F-measure. The false positive rate refers to the probability that the system generates an alarm while there is no human motion in the area of interest. The false negative rate refers to the probability that the system fails to detect the human motion in any place in the area. We also use the F-measure, which provides a single value to measure the effectiveness of the detection system [31].

Since each anomalous sample may not be detected simultaneously, we also studied the detection latency, i.e. how much time the system needs to associate an anomalous

Table I

SYSTEM PERFORMANCE UNDER THE SAME PARAMETERS
($l = 5, \alpha = 0.01, l_{\text{UPDATE}} = 15$) FOR THE TWO TESTBEDS.
ENHANCEMENT IS WITH RESPECT TO THE F-MEASURE OF THE BASIC
DETECTION MODULE.

		Basic Detection Module	Normal Profile Update Module	Decision-Refine-ment Module (**RASID Perf.**)
Testbed 1	FN Rate	0.0672	0.0876	**0.0468**
	FP Rate	0.2158	0.1176	**0.0378**
	F-measure	0.8683	0.8989	**0.9574**
	Enhancement	-	3.52%	**10.26%**
Testbed 2	FN Rate	0.2368	0.2069	**0.0966**
	FP Rate	0.1059	0.0903	**0.0372**
	F-measure	0.8167	0.8422	**0.9311**
	Enhancement	-	3.1%	**14%**

(a) False negative rate (b) False positive rate

Figure 10. Analysis of the Basic Detection Module parameters for Testbed 1.

Figure 11. Effect of the update window size parameter (l_{update}).

Figure 12. Comparison between the starting profile, updated profile and the true profile for the sample variance of the AP4-MP3 stream at the end of Experiment 1. As shown, the updated and true profiles are almost congruent.

sample with a detected event. The overall 90th detection latency percentile in both testbeds was found to be less than one second. Due to space constraints, we report the accuracy results only.

C. System Performance

Table I summarizes the system performance for both testbeds ***using the same parameters*** for all modules. The table also shows the enhancement introduced by each module to show the robustness of the techniques.

1) Basic Detection Module: As mentioned earlier, this module requires the selection of the sliding window size l and the significance α. Figure 10 illustrates the effect of these parameters applied to Testbed 1. Similar performance has been observed for Testbed 2. The figure shows that choosing a too short window size will make the system less sensitive to human motion. On the other hand, choosing a very large window size will introduce a very high FP rate. For the significance parameter, as α decreases, the FP rate decreases and the FN rate slightly increases. This means that increasing the significance will result in less system sensitivity. Therefore, to balance the different performance metrics, we choose $l = 5$ and $\alpha = 0.01$.

Table I shows that Testbed 2 has a higher FN rate than Testbed 1 in the Basic Detection Module. This is due to the larger testbed area (i.e. less coverage) and the time needed to move between the floors in Testbed 2. This is significantly enhanced by the processing performed by the Normal Profile Update and Decision Refinement modules. It can be noted also that the FP rate in Testbed 1 is relatively high. This is because the two-minute training period is not enough to sustain accurate detection for one hour of accurate operation inside the office environment. This highlights the need for the *Normal Profile Update Module*.

2) Normal Profile Update Module: The Normal Profile Update Module requires the selection of the update window size l_{update}. Choosing a too small l_{update} will make the system very sensitive to noisy readings causing a high FP rate. On the other hand, a very large l_{update} will make the system less sensitive to human motion causing a higher FN rate.
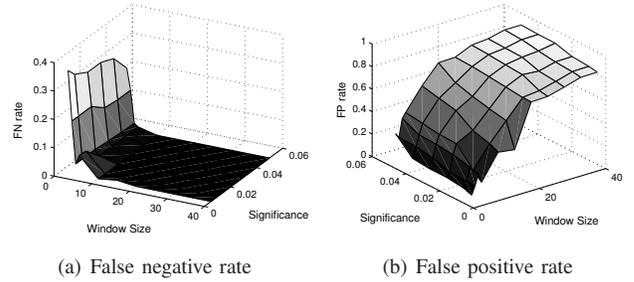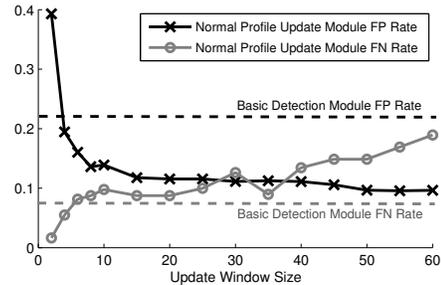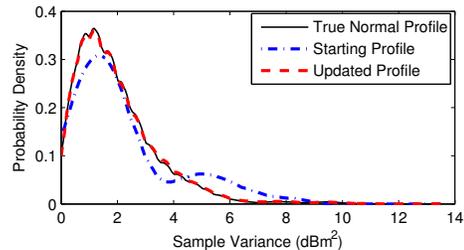
Figure 11 illustrates these effects of the update window size on the system performance for Testbed 1 when $l = 5$ and $\alpha = 0.01$. The figure shows that an update window size between 10 and 20 is sufficient to reduce the high FP rate without causing much increase to the FN Rate. Thus, we choose $l_{update} = 15$. The results are shown in Table I. The table shows that there is about 50% reduction in the FP rate in the first testbed, but this lead to a slight growth in the FN rate. For Testbed 2, the results of both the FN and the FP rates were enhanced due to adapting to the environment. Overall, the F-measure was enhanced by 3 to 4% with respect to the Basic Detection Module performance.

This enhancement can be explained by the observation that the Normal Profile Update Module reduces the effect of the temporal variations between the environment true normal

profiles and the stored normal profiles by updating them. We verified that by applying the two-sample Kolmogorov-Smirnov test to the distributions of the updated profiles and the distributions of the true normal state. The test accepted the hypotheses that those distributions came from the same underlying distribution at a significance of 0.05. Figure 12 provides an example comparing the starting, updated and true sample variance profiles at the end of Experiment 1.

3) Decision Refinement Module: This module fuses the data from all streams. Figure 6 displays the sum of anomaly scores curve for the data collected for Testbed 1. To reduce the FP rate, the curve is exponentially smoothed with a smoothing coefficient of 0.04. A large increment in the smoothed curve, by more than 20% to 25% from the normal level, implies a period of human motion. Our experiments show that deviations from these parameters values will not lead to significant degradation in the results. The figure shows that the motion periods are clearly distinguishable from the silence state. Table I shows that this module can lead to up to 10 to 14% enhancement in the F-measure for both testbeds with respect to the Basic Detection Module. It is important to note that this module also reduced the FN rate, as some of the previously undetected events are now detected because this technique makes use of the history of the state of the activity as described earlier.

D. Comparison with Previous Techniques

In this section, we compare the performance of *RASID* to the previous techniques devised for WLAN *DfP* detection: the moving average (MA) and moving variance (MV) techniques proposed in [14], and the maximum likelihood estimation (MLE) technique proposed in [15].

1) Comparison Aspects:

- Static accuracy: accuracy when the system is evaluated with the same profiles it was trained on (if any). This is to test the best attainable accuracy.
- Profiles' robustness: that is how consistent the performance of the system is when the tested profiles are different from the trained ones, for example due to temporal changes in the environment. For this case, the testing data set is collected two weeks after the data sets used for training.
- Overhead: the effort needed to deploy the system.

2) Comparison Results: Table II shows the comparison results in two cases.

In terms of the static accuracy, the results show that the F-measure of the *RASID* system is better than other systems in Testbed 1 and is slightly lower than the MLE technique in Testbed 2. Compared to the MA and MV techniques, the *RASID* system provides high accuracy due to the techniques it uses to enhance the performance. On the other hand, the MLE technique achieves slightly higher accuracy in Testbed 2 as it stores a motion profile, which requires much higher overhead than the *RASID* system.

		Results with static profiles			
		MA	MV	MLE	*RASID*
Testbed 1	FN Rate	0.1446	0.1426	0.0363	0.0468
	FP Rate	0.1385	0.104	0.1547	0.0378
	F-measure	0.858	0.8743	0.9099	**0.9574**
Testbed 2	FN Rate	0.0759	0.308	0.0372	0.0966
	FP Rate	0.7412	0.1478	0.0774	0.0372
	F-measure	0.6935	0.7522	**0.9438**	0.9311
	Overhead	No overhead	Minimal	Worst	Minimal
		Results with testing profiles separated two weeks from the training profiles.			
		MA	MV	MLE	*RASID*
Testbed 1	FN Rate	0.2165	0.319	0.1653	0.0472
	FP Rate	0.0711	0.1561	0.952	0.0782
	F-measure	0.8449	0.7414	0.5991	**0.9383**
Testbed 2	FN Rate	0.2641	0.4152	0.1203	0.0931
	FP Rate	0.3602	0.0513	0.831	0.0722
	F-measure	0.7022	0.7149	0.6491	**0.9165**
	Overhead	No overhead	Minimal	Worst	Minimal

In terms of profiles' robustness, the MA technique does not store any profiles. Therefore, its overall performance is low but almost the same as the profiles change. On the other hand, the robustness of the MLE technique is the least as it uses the mean signal strength values as the features used for classification. Therefore, after two weeks, the distribution of the signal strength does not follow the learned one. This is why the FP rate for the MLE technique is too high due to the shift that occurred in the signal distributions. It can also be noted that *RASID* performance in the two cases was the best because *RASID* uses the variance for its operation (dispersion feature) and employs techniques for adapting to changes in the environment and for enhancing the performance. This is why *RASID* performance is better than the MV in general, although the MV uses the same feature as *RASID*.

In terms of overhead, the MA technique has the minimum overhead as it does not need any learning phase. The MV and *RASID* deployment need to construct normal profiles by collecting samples for two minutes when the human is not present. On the other hand, the MLE technique has the worst overhead as it constructs motion profile at each location in the area of interest in addition to the normal profile.

In summary, although the static detection accuracy of *RASID* is as accurate as the MLE technique, the MLE technique has significantly higher overhead than *RASID* because of its motion profile requirements. In addition, *RASID* is the most robust technique to temporal changes in the training profiles and significantly outperforms the remaining techniques.

V. COMPARISON WITH A PARAMETRIC APPROACH

In this section, we compare the performance of the system's non-parametric approach to an analytical model that models the sample variance parametrically. The results of this model can help validate the results of our parameter

analysis in the previous section and can also motivate the usage of the non-parametric density estimation. The next evaluation will be based on the results of the Basic Detection Module only, so as to evaluate the two approaches without the enhancements. First, we describe the analytical model, then we present the results of the comparison.

A. The parametric model

The sample variance can be modeled parametrically given some conditions. According to Cochran's Theorem [32], the sample variance of l independent normally distributed random samples follows a chi-square distribution with $l-1$ degrees of freedom such that $\frac{(l-1)s^2}{\sigma^2} \sim \chi^2_{l-1}$, where σ^2 is the population variance. According to [33], the signal strength readings (in dBm) distributions for a stream j can be assumed to follow a normal distribution. Given that assumption, a parametric model can be devised for the system when the sample variance is used. Given a significance α and a window size l, the upper bound for the sample variance observed during the monitoring phase is $\chi^2_{l-1,1-\alpha}$. However, [33] also stated that the normality assumption may not hold in some cases. In addition, the signal strength readings may not be independent [34]. Thus, we believe that the non-parametric model described before will provide better performance than the parametric model. This will be verified in the following subsection.

B. Analysis Results

First, to check how close the parametric model is to the actual system, we compare the critical upper bounds obtained by both methods. For example, in Figure 13 we compare the critical sample variance values in both cases for the stream AP4-MP3 from Experiment 1, when the population variance is assumed to be 2.02 dBm^2 which is an experimental estimate for the population variance of that stream. The figure shows that the parametric model and the actual system critical values follow the same trends. However the difference between the curves suggests that the real case does not exactly follow the assumed parametric model. In addition, the effects of Basic Detection Module parameters can be inferred from the parametric model curves. As the window size parameter l increases, the critical variance value decreases which results in increased system sensitivity (i.e. higher FP rate and lower FN rate). Also, as the significance parameter α increases, the critical variance value decreases which also results in increased sensitivity. This is consistent with the analysis presented in Figure 10.

The next point is to study how the usage of the parametric model instead of non-parametric estimation can affect the system performance. As the distribution of the sample variance depends on the population variance, we analyze its effect. Figure 14 shows the effect of the population variance on the performance of the Basic Detection Module when the parametric model is used for Experiment 1. From the
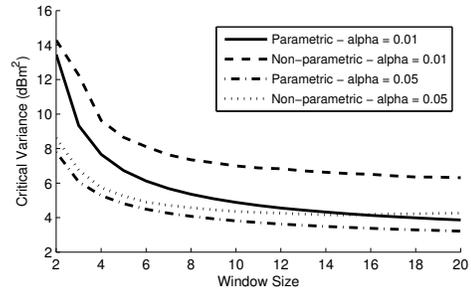

Figure 13. Comparison of the critical variance values of the parametric model and the *RASID* system model (non-parametric approach).
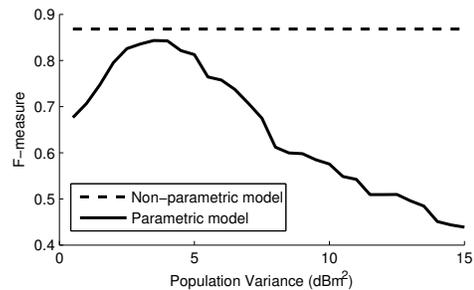

Figure 14. The performance of the Basic Detection Module when the parametric model is used versus the population variance, given $l = 5$ and $\alpha = 0.01$. The best population variance configuration provides an F-measure of 0.843 compared to 0.8683 that was obtained using the non-parametric estimation.

figure, we can conclude that the best performance achieved in terms of the F-measure (0.843) is less than the F-measure obtained using non-parametric estimation (0.8683).

To conclude, the parametric model leads to lower performance compared to the non-parametric estimation because the assumptions that the signal strength values are independent and follow a normal distribution may not hold. Also, the parametric model requires the selection of an accurate population variance. This cannot be done accurately without training for long time periods. Therefore, we conclude that *RASID* approach of constructing non-parametric profiles in a short offline phase and updating them in the online phase does provide a better option.

VI. CONCLUSIONS AND FUTURE WORK

In this paper, we presented the *RASID* system, a system that enables device-free passive motion detection using the already installed wireless networks. *RASID* uses non-parametric statistical anomaly detection techniques to provide the detection capability. The *RASID* system also employs profile update techniques to capture changes in the environment and to enhance the detection accuracy. The system was evaluated in two different real environments. Using the same parameters for the two testbeds, the system provided an accurate detection capability reaching an F-measure of at least 0.93 in both testbeds. The performance

of the *RASID* system was compared to the previously introduced techniques for WLAN *DfP* detection. The results showed that the *RASID* system outperformed the state-of-the-art techniques in terms of robustness and accuracy. In addition, we showed that the non-parametric approach employed by *RASID* has significant advantages over a parametric approach for the system operation.

Currently, we are expanding *RASID* in several directions: One direction is to integrate *RASID*'s detection capability with *DfP* tracking systems while considering larger testbeds. Another direction is to study possible sources of noise in typical wireless environments, e.g. other devices inside or outside the area of interest, and how to reduce their effect. We are also studying how the detected entity's characteristics, e.g. size, shape and motion pattern, can affect the system performance. Moreover, the site configuration, i.e. the positions of the APs and MPs, can also be studied in order to optimize the system performance.

ACKNOWLEDGMENT

REFERENCES

[1] P. Enge and P. Misra, "Special Issue on Global Positioning System," in *Proceedings of the IEEE*, January 1999, pp. 3–172.

[2] N. B. Priyantha, A. Chakraborty, and H. Balakrishnan, "The Cricket Location-Support System," in *MobiCom '00: Proceedings of the 6th Annual International Conference on Mobile Computing and Networking*, New York, NY, USA, 2000, pp. 32–43.

[3] R. Want, A. Hopper, V. Falcao, and J. Gibbons, "The Active Badge Location System." *ACM Trans. Inf. Syst.*, vol. 10, no. 1, 1992.

[4] M. A. Youssef and A. Agrawala, "The Horus WLAN Location Determination System," in *Communication Networks and Distributed Systems Modeling and Simulation Conference*, 2005, pp. 205–218.

[5] J. Krumm, L. Williams, and G. Smith, "SmartMoveX on a Graph - An Inexpensive Active Badge Tracker," in *UbiComp '02: Proceedings of the 4th International Conference on Ubiquitous Computing*, 2002.

[6] C. Randell and H. Muller, "Context Awareness by Analyzing Accelerometer Data," in *ISWC '00: Proceedings of the 4th IEEE International Symposium on Wearable Computers*, 2000, pp. 175–176.

[7] L. Bao and S. S. Intille, "Activity Recognition from User-annotated Acceleration Data," in *Pervasive Computing (LNCS)*, vol. 3001, 2004.

[8] M. Philipose, K. P. Fishkin, M. Perkowitz, D. J. Patterson, D. Fox, H. Kautz, and D. Hahnel, "Inferring Activities from Interactions with Objects," *IEEE Pervasive Computing*, vol. 3, October 2004.

[9] M. Wallbaum and S. Diepolder, "A Motion Detection Scheme For Wireless LAN Stations," in *Proceedings of the 3rd International Conference on Mobile Computing and Ubiquitous Networking*, 2006.

[10] J. Krumm and E. Horvitz, "LOCADIO: Inferring Motion and Location from Wi-Fi Signal Strengths," 2004, pp. 4–13.

[11] K. Kleisouris, B. Firner, R. Howard, Y. Zhang, and R. P. Martin, "Detecting Intra-room Mobility with Signal Strength Descriptors," in *MobiHoc '10: Proceedings of the Eleventh ACM International Symposium on Mobile Ad Hoc Networking and Computing*, 2010.

[12] I. Anderson and H. Muller, "Context Awareness via GSM Signal Strength Fluctuation," in *Pervasive 2006, Late Breaking Results*, 2006.

[13] T. Sohn, A. Varshavsky, A. Lamarca, M. Y. Chen, T. Choudhury, I. Smith, S. Consolvo, J. Hightower, W. G. Griswold, and E. D. Lara, "Mobility Detection Using Everyday GSM Traces," in *Ubicomp '06: Proceedings of the Eighth International Conference on Ubiquitous Computing*, 2006, pp. 212–224.

[14] M. Youssef, M. Mah, and A. Agrawala, "Challenges: Device-free Passive Localization for Wireless Environments," in *MobiCom '07: Proceedings of the 13th Annual ACM International Conference on Mobile Computing and Networking*. ACM, 2007, pp. 222–229.

[15] M. Moussa and M. Youssef, "Smart Devices for Smart Environments: Device-free Passive Detection in Real Environments," in *IEEE PerCom Workshops*, 2009.

[16] A. E. Kosba, A. Abdelkader, and M. Youssef, "Analysis of a Device-free Passive Tracking System in Typical Wireless Environments ," in *NTMS '09: Proceedings of the 3rd International Conference on New Technologies, Mobility and Security*, 2009, pp. 291–295.

[17] M. Seifeldin and M. Youssef, "A Deterministic Large-scale Device-free Passive Localization System for Wireless Environments," in *PETRA '10: Proceedings of the 3rd International Conference on Pervasive Technologies Related to Assistive Environments*, 2010.

[18] M. A. Seifeldin, A. F. El-keyi, and M. A. Youssef, "Kalman filter-based tracking of a device-free passive entity in wireless environments," in *WiNTECH'11: Proceedings of the 6th ACM International Workshop on Wireless Network Testbeds, Experimental Evaluation and Characterization*. New York, NY, USA: ACM, 2011, pp. 43–50.

[19] J. Krumm, S. Harris, B. Meyers, B. L. Brumitt, M. Hale, and S. A. Shafer, "Multi-Camera Multi-Person Tracking for Easyliving," in *Proceedings of the Third IEEE International Workshop on Visual Surveillance*, 2000, pp. 3–10.

[20] J. Wilson and N. Patwari, "Radio Tomographic Imaging with Wireless Networks," *IEEE Transactions on Mobile Computing*, May 2010.

[21] R. J. Orr and G. D. Abowd, "The Smart Floor: A Mechanism for Natural User Identification and Tracking," in *Proceedings of ACM CHI 2000 Conference on Human Factors in Computing Systems*, vol. 2, 2000.

[22] A. E. Kosba, A. M. Saeed, and M. A. Youssef, "Robust WLAN Device-free Passive Motion Detection," in *Proceedings of the IEEE Wireless Communications and Networking Conference, 2012*.

[23] S. S. Ram, Y. Li, A. Lin, and H. Ling, "Human Tracking Using Doppler Processing and Spatial Beamforming." IEEE Radar Conference, 2007.

[24] D. Zhang, J. Ma, Q. Chen, and L. M. Ni, "An RF-Based System for Tracking Transceiver-Free Objects," in *PerCom '07: Proceedings of the Fifth IEEE International Conference on Pervasive Computing and Communications*, 2007, pp. 135–144.

[25] A. L. AlHusseiny, M. Youssef, and M. ELTowiessy, "WCPS-OSL: A wireless cyber-physical system form object sensing and localization," in *The Workshop on Collaborative, Autonomic, and Resilient Defenses for Cyber Physical Systems (CyPhyCARD'11), in conjunction with CollaborateCom 2011*.

[26] N. Kassem, A. E. Kosba, and M. Youssef, "RF-based vehicle detection and speed estimation," in *VTC'12-Spring: Proceedings of the 75th IEEE Vehicular Technology Conference, 2012*.

[27] A. Eleryan, M. Elsabagh, and M. Youssef, "Synthetic Generation of Radio Maps for Device-free Passive Localization," in *Proceedings of the 54th IEEE Global Communications Conference, 2011*.

[28] B. W. Silverman, *Density Estimation for Statistics and Data Analysis*. Chapman & Hall/CRC, April 1986.

[29] D. W. Scott, *Multivariate Density Estimation: Theory, Practice, and Visualization*. Wiley, 1992.

[30] A. Rahim, S. Zeisberg, M. Fernandez, and A. Finger, "Impact of People Movement on Received Signal in Fixed Indoor Radio Communications," in *Proceedings of the 17th IEEE International Symposium on Personal, Indoor and Mobile Radio Communications*, 2006.

[31] C. J. V. Rijsbergen, *Information Retrieval*, 2nd ed. Newton, MA, USA: Butterworth-Heinemann, 1979.

[32] W. Cochran, "The Distribution of Quadratic Forms in a Normal System with Applications to the Analysis of Covariance," in *Mathematical Proceedings of the Cambridge Philosophical Society*, 1934.

[33] K. Kaemarungsi and P. Krishnamurthy, "Modeling of Indoor Positioning Systems based on Location Fingerprinting," in *INFOCOM 2004. Twenty-third Annual Joint Conference of the IEEE Computer and Communications Societies*, vol. 2, pp. 1012–1022.

[34] M. Youssef and A. Agrawala, "Handling samples correlation in the Horus system," in *INFOCOM'04: Twenty-third Annual Joint Conference of the IEEE Computer and Communications Societies*.